Proceedings of the 10th World Congress on Civil, Structural, and Environmental Engineering (CSEE 2025)
Barcelona, Spain - April, 2025
Paper No. ICGRE 163
DOI: 10.11159/icgre25.163

Exploring Sustainable Solutions: Parametric Analysis and Machine Learning for Finger-Jointed Casuarina Glauca Beams

Mohamed Elnakeb[1], Maryam Elshanawany[1], Mohamed Sabik[1], Mohamed Said[1], Rawan Debdeb[1], Mohamed Darwish[1], Khaled Nassar[1], Mohamed Abouzeid[1]
[1]The American University in Cairo
New Cairo, Cairo, Egypt
mohamedelnakeb@aucegypt.edu; mariamshanawany@aucedgypt.edu; mohamedsabik@aucegypt.edu; msaif9@aucegypt.edu; rawandebdeb@aucegypt.edu; mdarwish@aucegypt.edu; knassar@aucegypt.edu; mnagiba@aucegypt.edu

Abstract **-** The construction industry is responsible for approximately 39% of global carbon dioxide emissions, driven by the energy-intensive production of materials like cement and steel, as well as resource-depleting practices that contribute to deforestation, biodiversity loss, and pollution. To mitigate this environmental impact, the adoption of sustainable construction materials is critical. Casuarina Glauca, a hardwood species, emerges as a promising alternative due to its eco-friendly nature, high mechanical strength, and availability in regions with arid climates. However, its short timber lengths (0.8–1.2 m) limit its direct application in structural framing. This study explores the use of adhesive-reliant finger joints to address this limitation, enabling the creation of longer beams while retaining environmental benefits. A parametric analysis using finite element modelling in Abaqus was conducted to optimize joint configuration, amplitude, finger density, and adhesive type. Results show that increasing finger count (up to 16 per 10 cm) and amplitude (up to 50 mm) significantly enhances bending capacity, with Epoxy-bonded joints achieving up to 95% capacity, outperforming PVA-based alternatives. Additionally, a machine learning framework was developed to predict beam performance, leveraging models such as XGBoost, which achieved an R^2 of 0.9263 and RMSE of 0.0329. This predictive approach enables efficient design optimization, minimizing resource consumption and reducing testing costs. By combining numerical modelling and machine learning, this research addresses the limitations of Casuarina Glauca, promoting its use as a sustainable, high-performance material in construction. These findings pave the way for reducing construction-related emissions and costs while advancing eco-friendly engineering solutions.

Keywords: Sustainable Construction, Casuarina Glauca, Finger-Jointed Beams, Finite Element Modelling, Machine Learning

1. Introduction

The construction industry significantly contributes to environmental degradation, being responsible for nearly 39% of global carbon dioxide emissions. This high environmental impact stems from the extensive energy consumption and greenhouse gas emissions associated with the production of cement, steel, and other building materials [1]. Additionally, construction practices deplete natural resources, leading to deforestation, biodiversity loss, and pollution. Addressing these challenges requires urgent action to incorporate sustainable methods and materials that minimize environmental harm [2].

Green construction materials, derived from renewable resources with low carbon footprints, have emerged as viable alternatives to traditional materials. These include bamboo, rammed earth, and engineered wood, all of which offer lower embodied energy and promote circularity in construction [3]. The use of such materials not only reduces greenhouse gas emissions but also improves building energy efficiency, contributing to more sustainable construction practices [4].

Machine learning (ML) has emerged as a powerful tool in predicting the mechanical properties of materials, revolutionizing traditional experimental and computational approaches. By leveraging large datasets and advanced algorithms, ML can accurately predict material behaviour under various conditions, significantly reducing the need for extensive physical testing. This capability is especially valuable for novel materials or underexplored resources, where experimental data is scarce or costly to obtain. The integration of ML into materials science accelerates innovation, optimizes material performance, and fosters the development of sustainable construction practices by minimizing resource consumption and environmental impact [5].

Casuarina Glauca, a hardwood species, presents itself as a promising green construction material due to its unique properties and environmental advantages. Widely available in hot-climate regions like Egypt, it thrives in arid, nutrient-poor soils and can grow using wastewater, making it an eco-friendly and resilient resource [4]. Furthermore, Casuarina Glauca exhibits strong mechanical properties, such as high tensile and compressive strength, which make it suitable for various structural applications. Its use in construction aligns with the principles of sustainability, promoting locally sourced and renewable materials

Despite its advantages, Casuarina Glauca has a significant limitation: the short lengths of its timber, which range from 0.8 to 1.2 meters. These dimensions restrict its use in structural framing applications, where longer beams are typically required. This limitation can be addressed by employing adhesive-reliant finger joints to join shorter pieces into longer, structurally sound beams. This method enhances the applicability of Casuarina Glauca in structural construction while retaining its environmental benefits [6]

Existing literature highlights a gap in research on the parametric analysis of finger-jointed Casuarina Glauca beams using finite element modeling. While studies have explored the mechanical properties of the wood, none have investigated the effects of joint configuration, pitch, depth, and adhesive type on the structural performance of finger joints. This study aims to fill this gap by conducting a detailed parametric study using Abaqus software to optimize these parameters and develop cost-effective, high-performance beams. Additionally, a machine learning model will be developed to predict the bending capacity of the finger-jointed beams based on the stated parameters, providing a fast and accurate tool for performance evaluation and aiding in the design and optimization of such beams.

The findings of this research are anticipated to significantly enhance the utilization of Casuarina Glauca in structural applications. By addressing its length limitations and optimizing finger joint performance, this study will promote the adoption of this material as a sustainable and cost-effective alternative to conventional construction materials, leading to reduced carbon emissions and construction costs

2. Materials and Methodology

2.1. Materials

2.1.1. Casuarina Glauca

The study conducted by Hussein et al. [7] focused on the mechanical properties of Casuarina Glauca, a hardwood species commonly found in Egypt. A series of tests, including compression (parallel and perpendicular to the grain), static bending, tension (parallel and perpendicular to the grain), and cleavage, were performed in accordance with ASTM standards. The results revealed that Casuarina Glauca possesses high mechanical strength and ductility, making it a promising material for structural applications. Its performance was comparable to or exceeded that of many hardwoods traditionally used in construction, demonstrating its potential as an alternative for various structural uses.

Table 1: Mechanical Properties of Casuarina Glauca

Material Property	Value
Compression Parallel to Grain (MPa)	32.2
Compression Perpendicular to Grain (MPa)	7.4
Bending Modulus of Rupture (MPa)	62.1
Tension Parallel to Grain (MPa)	162.9
Tension Perpendicular to Grain (MPa)	5.9
Cleavage Strength (MPa)	0.8
Modulus of Elasticity (MPa)	716.4 (Tension Parallel)

2.1.2. Adhesives

Epoxy resin and polyvinyl acetate (PVA) adhesives are extensively utilized in various applications due to their distinct mechanical properties. Epoxy resins are renowned for their high tensile and compressive strengths, making them suitable for structural applications. For example, tensile strengths ranging from 60 to 80 MPa and compressive strengths between 90 and 120 MPa have been reported for epoxy resins [8] .These properties arise from their thermosetting polymer structure, which provides excellent bonding strength and durability. In contrast, PVA adhesives, while offering adequate tensile strengths of 3 to 5 MPa for woodworking and paper bonding, exhibit lower mechanical strength overall.

Mechanical properties are determined through standardized tests. For example, tensile strength is measured using ASTM D638 or ISO 527 standards, where a sample is subjected to uniaxial tension until failure. Compressive strength is assessed following ASTM D695 or ISO 604, involving the application of uniaxial compressive force until the specimen fails**.** Shear strength, critical for adhesive applications, is evaluated using ASTM D1002 or ISO 4587, where bonded assemblies are subjected to shear loading until failure.

Table 2: Mechanical Properties of Adhesives

Mechanical Property	Epoxy Resin	PVA Adhesives
Tensile Strength (MPa)	60-80	3-5
Compressive Strength (MPa)	90-120	5-10
Shear Strength (MPa)	25-30	2-4

2.2. Methodology
2.2.1. Numerical Analysis

The process of conducting a finite element analysis (FEA) using ABAQUS software, as illustrated in the flowchart, involves a comprehensive series of steps designed to ensure accuracy and reliability. The first step is defining the material properties, which include both elastic and plastic characteristics. Elastic properties, such as the modulus of elasticity (E), are critical as they define the stress-strain relationship in the linear elastic range. The modulus of elasticity is determined using Hooke's Law, expressed as:

$$\boldsymbol{\sigma} = \boldsymbol{E} \cdot \boldsymbol{\varepsilon} \tag{1}$$

,where σ is the stress, E is the modulus of elasticity, and ε is the strain.

Next, the plastic properties are defined, focusing on plastic strain εp, which is the permanent strain remaining after unloading. The relationship for plastic strain is described as:

$$\boldsymbol{\varepsilon} = \boldsymbol{\varepsilon e} + \boldsymbol{\varepsilon p} \tag{2}$$

,where **ε** is the total strain, εp is the elastic strain, and εp is the plastic strain. The plastic behaviour is modelled using yield criteria of von Mises. Damage evolution, particularly in fracture-prone materials, is characterized by fracture energy (Gf), representing the energy required for crack propagation per unit area, obtained from the stress-strain curve of the material. ABAQUS incorporates damage initiation criteria (e.g., maximum stress or strain) and damage evolution laws to model stiffness degradation after initiation. Contact behavior between parts is another key factor. ABAQUS simulates cohesive behavior to model bonding and debonding, starting with damage initiation at a critical stress (σc) or strain (εc). Damage evolution, governed by fracture energy, describes bond degradation until complete separation, with cohesive elements ensuring accurate interaction modeling. The process includes defining material properties, creating part geometries, assembling components, applying boundary conditions and loads, and generating a mesh. Calibration ensures alignment with experimental or theoretical results, followed by validation against independent criteria, ensuring model reliability for structural analysis. This iterative approach creates a robust FEA model [9].

The parametric study investigates factors affecting finger-jointed *Casuarina Glauca* beams, including finger joint amplitude, joint density, and configuration (traditional, flipped, or separated). Adhesive type (Epoxy or PVA) is also critical for bonding strength, as shown in Figure 1.

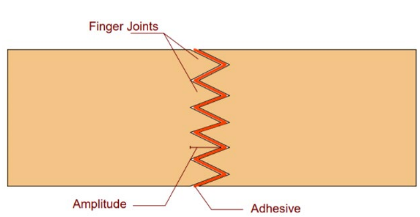

Figure 1. Finger Jointed Beam Parameters Illustration

Each parameter is varied systematically, as shown in Figure 2, to evaluate its impact on the bending capacity and structural performance. For instance, higher amplitudes and increased finger counts generally improve load-bearing while joint configurations affect stress distribution. These parameters were modeled and analyzed using finite element software, enabling a comprehensive understanding of their influence on beam optimization.

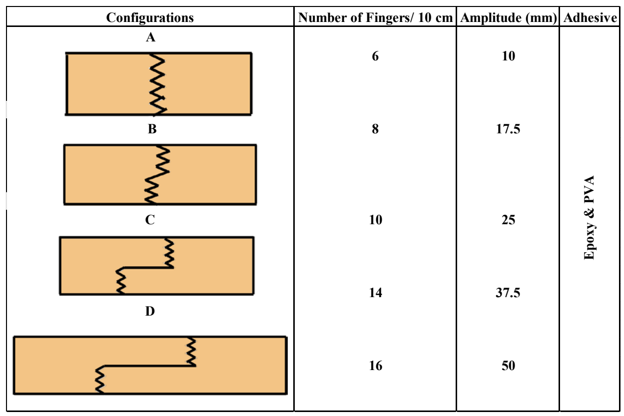

Figure 2. Finger Jointed Beam Parameters Illustration

2.2.2. Machine Learning

Figure 3. Machine Learning Methodology Framework

The methodology follows the framework outlined in Figure 3, starting with preliminary machine learning models like Decision Tree, Random Forest, and Linear Regression in their default configurations. These baseline models provide an initial understanding of the dataset's behavior and predictive potential, highlighting key insights and challenges such as overfitting, underfitting, or feature significance. This step informs subsequent data refinement and model development. The data preparation phase involves cleaning and preprocessing to ensure reliability, including the removal of invalid or non-numeric entries (e.g., in column TL), eliminating irrelevant features, and encoding categorical variables using techniques like binary, ordinal, and one-hot encoding.

To enhance the dataset, techniques such as standard and Min-Max scaling normalize numerical features, while logarithmic and square root transformations address skewness and outliers. Outliers in the target variable are identified and removed using statistical methods to prevent distortion of results. Feature selection leverages gradient boosting to rank predictors, identifying the most influential ones for advanced model training. Refined data is used to train and optimize advanced models like XGBoost, LightGBM, and Random Forest, alongside simpler models like Decision Tree, through systematic hyperparameter tuning. Model performance is evaluated using RMSE and R^2 metrics: RMSE quantifies quantifies prediction errors, with lower values indicating better performance, while R^2 measures the proportion of variance variance explained by the model, with values closer to 1 reflecting a stronger fit. Together, these metrics provide a comprehensive view of model accuracy and reliability. The metrics are calculated as follows

$$RMSE = \sqrt{\frac{\sum_{i=1}^{n}(yi - yactual[i])^2}{n}} \tag{3}$$

$$R2 = 1 - \frac{\sum_{i=1}^{n}(yi - yactual[i])^2}{\sum_{i=1}^{n}(yi - ymean)^2} \tag{4}$$

3. Results and Discussion

3.1. Parametric Study

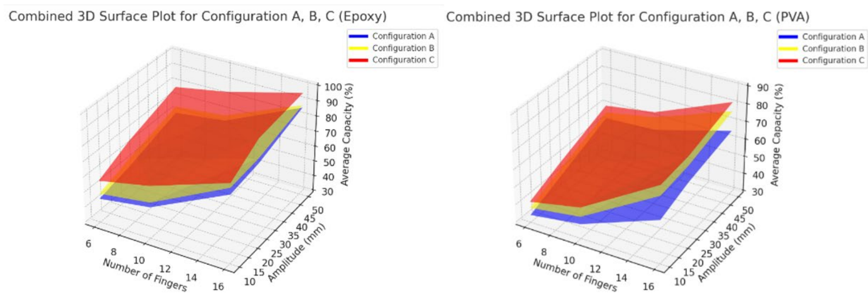

Figure 4. Surface Plot of Average Bending Capacity Percentage of Epoxy Finger-Jointed Beams

The presented Figure 4 and analysis highlight the significant effects of varying the number of fingers and the amplitude on the average capacity percentage for configurations utilizing both Epoxy and PVA as adhesives. The data demonstrates that increasing either parameter independently results in an enhancement of the average percentage capacity, with a particularly notable improvement observed when the number of fingers is increased. This indicates that the number of fingers is the more influential factor compared to amplitude in optimizing joint performance. Furthermore, the superiority of Epoxy as an adhesive is evident across all configurations, consistently yielding higher capacities than PVA. Among the three configurations examined, Configuration C exhibits the highest capacity, emphasizing its structural efficiency when paired with either adhesive. The results obtained surpass those reported in previous study by Darwish et al [6], where only a 30% capacity was achieved using PVA. The current study, however, demonstrates that capacities as high as 80% are attainable, particularly when optimizing both the number of fingers and amplitude in conjunction with using Epoxy. The combined effects of these parameters reveal a synergistic enhancement of capacity, underscoring the critical role of both design optimization and adhesive selection in achieving superior performance.

3.2. Machine Learning

3.2.1 Spearman Correlation Matrix

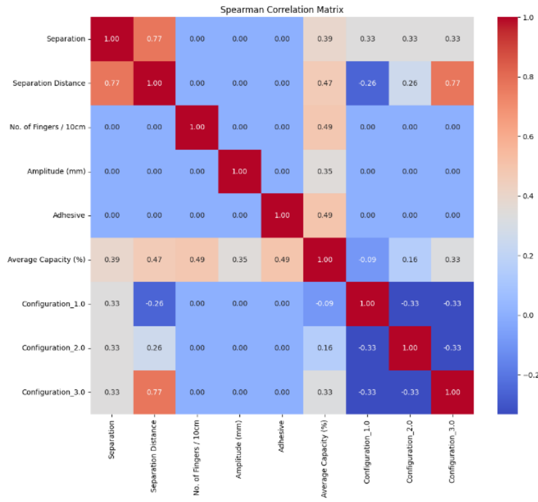

Figure 5. Spearman Correlation Matrix

The Spearman correlation matrix, as shown in Figure 5, provides insights into the relationships between key parameters affecting joint performance. A strong positive correlation (0.77) is observed between separation and separation distance, indicating that these factors are closely linked. The number of fingers shows a moderate positive correlation (0.49) with amplitude and adhesive, suggesting that increasing the number of fingers enhances the effectiveness of these parameters. Average capacity exhibits moderate positive correlations with the number of fingers (0.49) and adhesive (0.49), highlighting their significant contribution to joint strength. Notably, there is no strong correlation between configuration types, indicating distinct behaviour patterns across configurations.

3.2.2 Parameters Boxplots

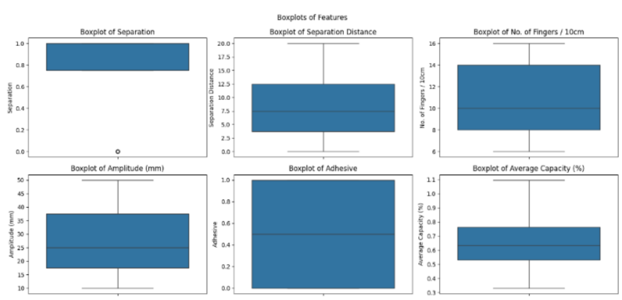

Figure 6. Boxplots of the Parameters

The boxplots, as shown in Figure 6, illustrate the distribution of key parameters and configurations. Separation shows minimal variability, while separation distance and the number of fingers exhibit broader distributions, indicating diverse parameter ranges. Amplitude displays a uniform spread with no extreme outliers, whereas average capacity shows a concentration around 70%, with moderate variability. Adhesive usage appears binary, likely reflecting the comparison of two types (Epoxy and PVA). Configurations 1.0, 2.0, and 3.0 show limited spread, with a few outliers, indicating specific dominant settings for each configuration.

3.2.3 Feature Selection

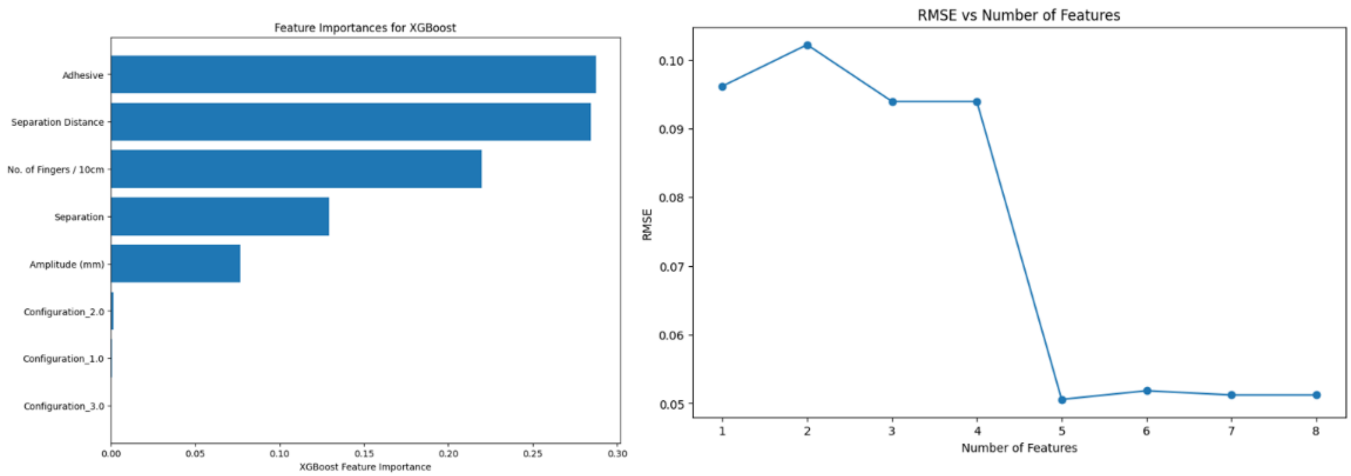

Figure 7. Feature Selection Plots

The feature importance plot, as shown in figure, highlights that adhesive, separation distance, and the number of fingers is the most significant contributors to model performance, with amplitude and separation having a smaller but notable impact. Configuration types have minimal influence. The RMSE plot demonstrates that the model's error decreases substantially as the number of features increases, with a sharp drop when incorporating the top four features. This emphasizes the critical role of these key parameters in accurately predicting the system's performance.

3.2.4 Evaluation Metrics

Table 3: Evaluation Metrics of the Different Machine Learning Models

Model	**R2**	**RMSE**
XGBoost	0.9263	0.0329
Light GBM	0.8927	0.0397
Random Forest	0.8502	0.0470
Decision Tree	0.6059	0.0762
Linear Regression	0.6519	0.0716

The results demonstrate that XGBoost outperforms other models with an R^2 of 0.9263 and the lowest RMSE of 0.0329, indicating excellent predictive accuracy and minimal error. Light GBM and Random Forest also perform well, with R^2 values of 0.8927 and 0.8502, respectively, though their RMSE values are higher, reflecting slightly less precision. Decision Tree and Linear Regression show significantly lower R^2 values (0.6059 and 0.6519) and higher RMSE, making them less reliable for this application. XGBoost's superior performance is due to its ability to handle complex feature interactions and its regularization techniques, which prevent overfitting and enhance generalization, making it the best choice for this analysis.

3. Conclusions

- Casuarina Glauca exhibits outstanding mechanical properties, such as a bending modulus of rupture of 62.1 MPa and tensile strength parallel to the grain of 162.9 MPa, making it a viable alternative to traditional hardwoods for structural applications.
- Increasing the number of fingers (up to 16) and amplitude (up to 50 mm) significantly enhances the bending capacity of finger-jointed beams. Epoxy-bonded configurations achieved capacities up to 80%, demonstrating superior performance compared to PVA-bonded beams.

- The XGBoost machine learning model delivered the best predictive performance with an R^2 of 0.9263 and RMSE of 0.0329, validating its effectiveness in identifying key factors and predicting joint performance accurately.
- Adhesive type, number of fingers, separation distance, and amplitude are critical parameters influencing the performance of finger-jointed beams. Optimization of these parameters is essential to achieve maximum structural efficiency.
- The demonstrated mechanical performance and design optimizations open the possibility for increasing the length of structural beams. By leveraging advanced adhesives like Epoxy and refined joint configurations, longer and stronger beams can be developed for more demanding construction applications.

References

[1] IPCC, "Climate Change 2022: Mitigation of Climate Change," Geneva, Switzerland, 2022.

[2] G. K. C. Ding, "Sustainable construction—The role of environmental assessment tools," *J Environ Manage*, vol. 86, no. 3, pp. 451–464, Feb. 2008, doi: 10.1016/j.jenvman.2006.12.025.

[3] J. Zuo and Z.-Y. Zhao, "Green building research–current status and future agenda: A review," *Renewable and Sustainable Energy Reviews*, vol. 30, pp. 271–281, Feb. 2014, doi: 10.1016/j.rser.2013.10.021.

[4] M. M. Hussein, K. Nassar, and M. Darwish, "Design and Characteristics of a Novel Casuarina Glauca Wooden K-Truss Formwork," *Practice Periodical on Structural Design and Construction*, vol. 27, no. 3, Aug. 2022, doi: 10.1061/(ASCE)SC.1943-5576.0000694.

[5] Z. Song, X. Chen, F. Meng, G. Cheng, C. Wang, Z. Sun, and W.-J. Yin, "Machine learning in materials design: Algorithm and application," *Chinese Physics B*, vol. 29, no. 11, p. 116103, Nov. 2020, doi: 10.1088/1674-1056/abc0e3.

[6] M. Darwish, M. Adham, H. Allam, K. Yousri, and T. Hassan, "Design and Characteristics of a Single-Storey Hybrid Wood–Soil Structure," *Buildings*, vol. 14, no. 6, p. 1785, Jun. 2024, doi: 10.3390/buildings14061785.

[7] N. Abdellatif, M. Darwish, K. Nassar, P. Youssef, A. Dardir, A. Ahmed, M. Eltamimy, M. Mamdouh, and R. Abdelazim, "Manufacturing and Mechanical Testing of Casuarina Glauca Blockboards," in *Sustainable Issues in Infrastructure Engineering*, M. Darwish, Ed. Cham: Springer, 2021, pp. 14–22, doi: 10.1007/978-3-030-62586-3_2.

[8] M. Khalina, M. H. Beheshty, and A. Salimi, "The effect of reactive diluent on mechanical properties and microstructure of epoxy resins," *Polymer Bulletin*, vol. 76, no. 8, pp. 3905–3927, Aug. 2019, doi: 10.1007/s00289-018-2577-6.

[9] O. C. Zienkiewicz, R. L. Taylor, and J. Z. Zhu, *The Finite Element Method: Its Basis and Fundamentals*, 7th ed. Butterworth-Heinemann, 2005.